[UCI]I804:24011-200000264093

2013년 8월

석사학위 논문

Lowering LUMO Energy of Phenylated o-Carborane

조 선 대 학 교 대 학 원

화 학 과

황 조 현

Lowering LUMO Energy of Phenylated o-Carborane

2013년 8월 23일

조 선 대 학 교 대 학 원

화 학 과

황 조 현

Lowering LUMO Energy of Phenylated o-Carborane

지도교수 이 종 대

이 논문을 이학석사학위신청 논문으로 제출함.

2013년 4월

조 선 대 학 교 대 학 원

화 학 과

황 조 현

황조현의 석사학위논문을 인준함

위원장 조선대학교 교수 이 범 규 (인)

위 원 조선대학교 교수 이 종 대 (인)

위 원 조선대학교 교수 임 종 국 (인)

2013년 5월

조 선 대 학 교 대 학 원

TABLE OF CONTENTS

Lowering LUMO Energy of Phenylated o-Carborane

LIST OF FIGURES

Abstract

Lowering LUMO Energy of Phenylated o-Carborane

Hwang Johyun
Advisor : Prof. Lee Jong Dae, Ph.D,
Department of Chemistry,
Graduate School of Chosun University

전자 수용성은 두 개의 인접한 페닐-p* 탄소-s* 궤도 사이의 호의적인 전자 상호작용을 통해 B-phenylated tri-phenyl-o-carborane (1) 번은 크게 향상 되었다. 3번 위치 붕소 원자의 페닐 치환은 카본원자의 두 페닐그룹은 마주보는 위치로 이끈다. 그리고 최대치 LUMO 에너지 안정화를 주고 광범위한 전자 비편재화로 완고한 형태로 그것들을 묶어 놓는다. -1.72V에서 CV로부터 가역 환원 피크와 광대하고 연장된 UV 흡수 (l_{max}=277nm)는 LUMO 안정화와 o-carborane의 전자 수용성 같은 것을 설명하고 입증한다. $Cr(CO)_6$ 1번 화합물이 반응할 때 인접한 o-carborane으로 부터의 전자감소 때문에, 페닐 그룹은 인접하게 된다. 그래서 bimetallic chromium complex (4)는 크로늄 원자와 페닐그룹 사이에 h^6-bonding 방식으로 선택적으로 형성됐다.

1. Introduction

Electron accepting property of o-carborane[1] has been suggested and its application to electronic alteration has been a subject of interest in both organic[1a,b,d] and organometallic chemistry.[1c] However, other than reports of electron accepting property arisen from the organic substitution,[1a,b,d] detailed study that elaborates electron accepting property of o-carborane has not been properly made. Recently, o-carborane σ* orbital contributed mainly from cage carbons is greatly stabilized by the addition of adjacent phenyl groups2 alluding that o-carborane's electron accepting capability is the function of LUMO energy stabilization, perse. Granting that o-carboranyl C-C σ* orbital initiates electronic alteration to the π-system of the aromatic groups directly bonded, namely, through the π*channel, systematic investigation on LUMO energy is by all means important to uncover the origin of electron acceptor character of o-carborane. To this end, we have laid our eyes on the geometries governed by the substitution either by the carbon or the boron atom or both atoms.

2. Results and Discussion

Starting from mono-phenylated or di-phenylated o-carborane, 1-phenyl-(PhC) or 1,2-di-phenyl-o-carborane (Ph_2C_2), tri-phenylated 1,2,3-Ph3-C2B(**1**) and 1,2,6-Ph3-CB2(**2**) and tetra-phenylated 1,2,3,6-Ph4-C2B2(**3**) were prepared in moderate yields (37 ~86%).[3] As shown in Scheme 1, we first carried out phenyl substitutions on either/both 1,2-carbons or/and 3,6-borons of the icosahedral o-carborane framework (see details in supporting information).

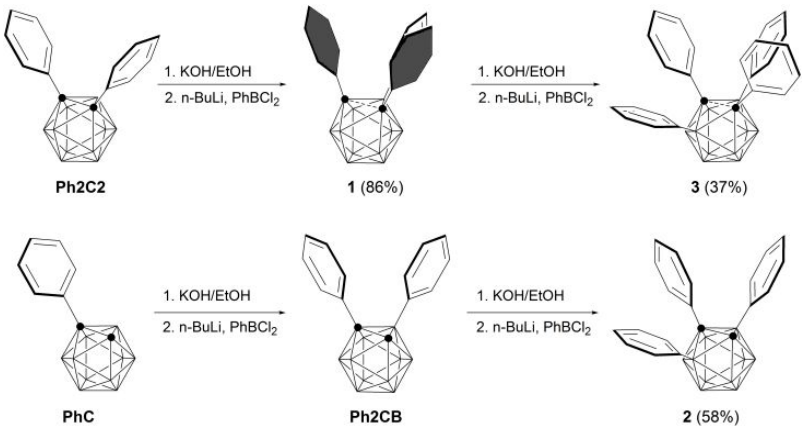

Scheme 1. Preparation of phenylated o-carboranes **1-3**

Depending on the substitution site either the boron or carbon atom, their ^{11}B NMR show either symmetric or asymmetric pattern;[4] most asymmetric one is Ph_2BC followed

by **1** and **2** in which two of them are related to the boron-substitution and the most symmetric one is tertra-phenylated compound (**3**)(see Figure S4-S9).

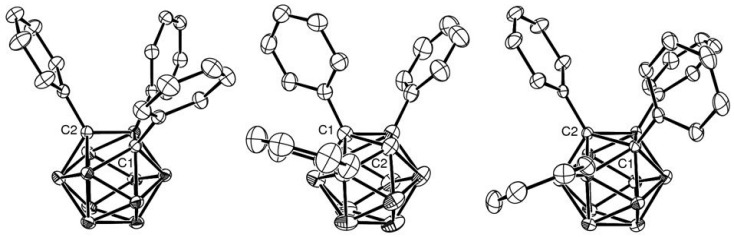

1 (1.763 Å) **2** (1.632 Å) **3** (1.704 Å)

Chart 1. Molecular structures of phenylated-o-carboranes **1**, **2**, and **3** which have been characterized by means of X-ray crystallography, respectively (see details in supporting information).

Single crystal X-ray structure determination clearly revealed structural authenticity of each compound and alluded electronic alteration via investigation on the C-C distance: C-C bond distance is a direct measure of electronic alteration because it reflects C-C σ* orbital's contribution and directly affected LUMO energy.[2] In this series, C-C distance is the longest for **1** followed by **3** and the shortest for **2**. **1** and **3** are further phenyl decoration at the boron atoms keeping Ph_2C_2 platform abreast while **2** contains one free phenyl carbon atom.[5] In line with expectation of C-C bond distance and LUMO energy stabilization, longer C-C bond correlates to larger LUMO contribution, vide infra. It is now obvious that placement of two phenyl groups at the carbon atoms

is the minimum requirement of LUMO stabilization and conformation of the two phenyl groups at the carbon atoms that fits well to the LUMO can contribute greatly to the stabilization of LUMO. As can be seen in Figure S1, structure of **1** has a special feature in which additional phenyl unit is substituted at the boron atom takes up a conformation to lock two phenyl group at the two carbon atoms into a rigid posture responsible for the LUMO stabilization. **2** does not possesses Ph_2C_2 platform, so LUMO stabilization is not seen. Finally, all phenylated to the neighboring boron atoms found in compound **3** do not show enough LUMO stabilization which indicates that favorable phenyl π^* and o-carboranyl C-C σ^* orbital interaction is not occurring in that conformation; indeed, in the solid structure, two phenyls at the carbons are not taking up the face-to-face conformation for the favorable interaction. All those can be summarized in dihedral angle between two phenyl rings with respect to the C-C vector in which larger dihedral angle gives rise to a face-to-face conformation and thus exhibits maximum C-C σ^* orbital interaction as found in **1** and **3**; dihedral angles of 88.73(6) and 67.06(1)° for **1** and **3**, respectively, can be accounted for the better orbital overlaps. However, smaller dihedral angle for **3** appears to be due to the steric interference by the B-phenyl groups.

From comparison between **1** and Ph_2C_2 shown in Figure 1, excitations are mainly from phenyl units depending much to the carbon atom substitution albeit with low intensities. Given the fact that single carbon substitution in PhC shows bathochromic shift arisen from the phenyl group,[6] further boron substitution does not exert much effect on the electronic structure alteration as found in the spectrum of **2**. This new find-

ing is ascribed to the new excited state arisen from the new electronically viable vibronic modes coupled with facing two phenyl π* orbitals at the carbon atom solely. It is clear now that one condition to be met allowing enhanced electron withdrawing capability of o-carborane is the special geometry preference with coupling accessible phenyl π* orbitals which is found in Ph_2C_2. As can be seen from the spectra of tri-phenyl substitution (**1**), further phenyl substitution on boron is much enhanced. From absorption spectra, forbidden symmetrical excitations belong to benzene are now somewhat relaxed when phenyl groups are emplaced to the carbon atoms of the o-carborane as found in **1** and **3**. It is now clear that **1**) "Ph_2C_2" unit is essential to lower LUMO energy and **2**) bathochromic shift is the revelation of extensive electronic coupling found in **1** and **3**.

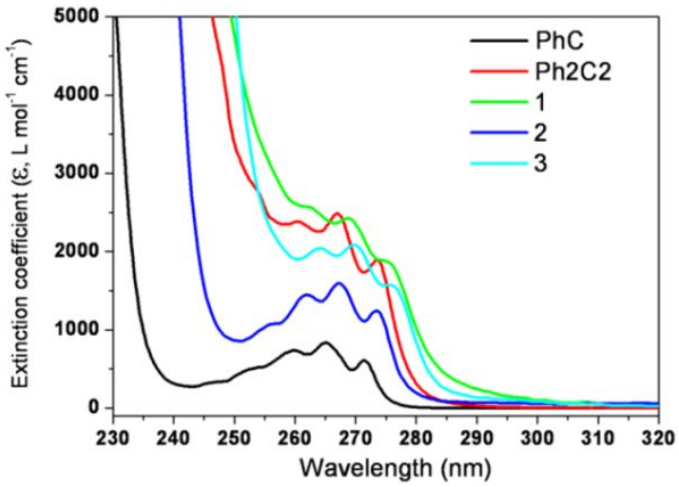

Figure 1. Absorption spectra of PhC, Ph_2C_2, **1**, **2**, and **3** in hexane solution at room temperature.

All other optical properties as well as electronic properties of CV data are now presented in the Table 1. There exists a strong correlation between the geometry and the electronic structure including optical spectroscopy.[2] When two carbon atoms are engaged with phenyl groups, most effectively by the bis-substitution at the carbon atoms, expected reversible reduction was observed.[2] Also, those values are the indication of electronic alteration and is proportional relationship to the degree of LUMO energy stabilization as found in CV reduction potentials for **1-3** by further phenyl-substitution.

Table 1. Physical Properties of Ph_2C_2 and 1- 4.

Comp	λ_{abs} (nm)[a] [ε, M^{-1},cm^{-1}]	λ_{em} (nm)[a]	E_{ox} (V)[c]	E_{red} (V)[c]
Ph_2C_2	224, 267, 273 [13713, 895, 737]	–[d]	–[d]	–2.05
1	227, 267, 277 [10423, 895, 751]	–[d]	–[d]	–1.72
2	223, 267, 277 [12114, 612, 692]	298	–[d]	–[d]
3	230, 267, 273 [11917, 795, 722]	301	–[d]	–2.25
4	257, 327, 405 [11713, 12783, 3421]	–[d]	0.49	–1.41

[a]Measured in Ar-saturated hexane solution (20 μM) at room temperature. [b]Taken by excitation at 270 nm. [c]Oxidation and reduction potentials measured for Ar-saturated dichloromethane solution by cyclic voltammetry (V vs SCE). [d] Not detected.

In view of effective LUMO stabilization of o-carboranyl C-C σ* orbital by two phenyl π* orbitals, organometallic π* donor group has been further introduced onto phenyl groups;[7] reaction of **1** with $Cr(CO)_6$ produced phenyl coordinated bis chromium complex (**4**) in good yield (see experimental details for the synthesis and X-ray structural determination data in Supporting Information). Lowered LUMO appeared to keen on allowing ideal coordination energy for π* donor, $Cr(CO)_3$, and with those Cr coordination even stabilized the LUMO of diphenyl-o-carborane was accomplished.

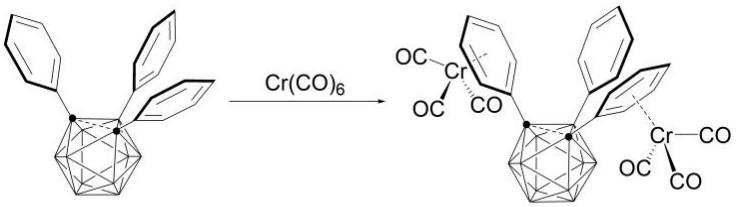

1 **4** (87%)

Chart 2. Preparation $Cr(CO)_3$ coordinated diphenyl-o-carborane and structure confirmed by X-raycrystallography in which C-C distance(1.777Å) showed the longest among **1-4**.

NMR spectra clearly showed the Cr coordination to the phenyl groups with the chemical shifts of δ 7.30 − 7.62 and 128.7 − 141.5 for ^{1}H and ^{13}C NMR, respectively. Coordinating to carbon phenyls was confirmed by X-raycrystallography. As expected, C-C distance is the longest with the value of 1.777 Å which lies essentially in the range of nonbonding.[8] Agreeing to the geometrical change, absorption responsible for the LUMO energy is now altered greatly to lower energy with a broad peak extending to 405nm. As shown in Figure 2, CV spectrum of **4** has one irreversible oxidation and one reversible reduction waves at 0.49 and −1.41 V, which correlate to the chromium (0/+1) metal center and the Ph_2C_2 unit, respectively. Comparing reduction potentials of the Ph_2C_2 unit for Ph_2C_2 and **1** and **4**, LUMO energy stabilization is clearly seen on going from Ph_2C_2 and **1** to **4**. Previously, the 5.78 eV of HOMO-LUMO gap of Ph_2C_2 was reported by measurement of the UV-Vis spectra. Time-dependent DFT (TD-DFT) calculation was performed on the optimized geometry of tri-phenyl-o-carboranes (**1-4**) and the resulting X-ray crystallographic structures are excellent agreement with those observed in the structures. As shown in Figure 2, the frontier orbitals of the tri-phenyl-o-carborane **1** is largely centered on the *B*-substituted phenyl ring, with the HOMO-LUMO gap (5.23 eV) accounting in part for the stability of this compound and the resulting simulated electronic spectra are in excellent agreement with those observed. In comparison to **1**, the optimized geometry for chromium complex **4** reveals that the compositions of the LUMO frontier orbitals are similar to those found in the optimized geometry for **1** and the small HOMO-LUMO gap (3.67 eV) accounting in part for the stability of this compound. The LUMO is

associated with *C*-substituted two phenyl rings and partially carborane and chromium metal atoms.

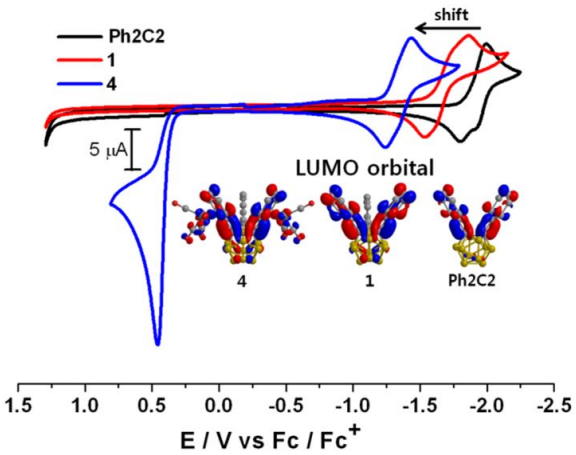

Figure 2. Cyclic voltammograms of Ph_2C_2, **1**, and **4** in CH_2Cl_2 solution (scan rate=100mV/s). (Inset: HOMO-LUMO frontier orbital analysis in the ground state)

3. Conclusion

We found that LUMO of Ph_2C_2 was stabilized through B-phenylation in **1** and tri-phenyl-o-carborane (**1**) functioned as strong p-acceptor to form a stable new types of organometallic complex (**4**) through Cr(d)-Ph(π*)-o-carboranyl C-C (σ*)metal to ligand back-bonding interaction. This study clearly shows the electron withdrawing property of o-carborane is evident as long as two phenyl groups are juxtaposed and paralleled.

4. Experimental Section

General Procedures. All manipulations were performed under a dry nitrogen or argon atmosphere using standard Schlenk techniques. Tetrahydrofuran (THF) was distilled under nitrogen from sodium/benzophenone. The elemental analyses were performed using a Carlo Erba Instruments CHNS-O EA 1108 analyzer. High Resolution Tandem Mass Spectrometry (Jeol LTD JMS-HX 110/110A) was performed at the Korean Basic Science Institute (Seoul). The ^{1}H, ^{11}B, and ^{13}C NMR spectra were recorded on a Varian Mercury 300 spectrometer operating at 300.1, 96.3, and 75.4 MHz, respectively. All 11B chemical shifts were referenced to $BF_3 \bullet O(C_2H_5)_2$ (0.0 ppm) with a negative sign indicating an up-field shift. All proton and carbon chemical shifts were measured relative to the internal residual $CHCl_3$ from the lock solvent (99.9% $CDCl_3$). The absorption and photoluminescence spectra were recorded on a SHIMADZU UV-3101PC UV-VIS-NIR scanning spectrophotometer and a VARIAN Cary Eclipse fluorescence spectrophotometer, respectively. The fluorescence lifetimes were measured by a time correlated single photon counting spectrometer. The emission quantum yields (ϕPL) of the carborane compounds were calculated by means of the comparative method of William1 for samples of five different concentrations (1 μM ~ 5 μM) using 9,10-diphenylanthracene (ϕPL = 0.95) and Rhodamine B (ϕPL = 1.00) as a reference standard. Decarborane, o-carborane, 1-phenyl-o-carborane were purchased from Katchem and N,N-dimethylaniline, dichlorophenylborane, n-BuLi (2.5 M in hexane), chromium hexacarbonyl complex ($Cr(CO)_6$) were purchased from Aldrich Chemicals.

Cyclic voltammetry and Spectroelectrochemistry. The cyclic voltammetry experiments were performed using a BAS 100 electrochemical analyzer. A three-electrode cell system containing a platinum disk, a platinum wire, and $Ag/AgNO_3$ as the working, counter, and reference electrodes, respectively, was used. All data were obtained for Ar-purged CH2Cl2 solution containing 0.1M tetrabutylammonium perchlorate (TBAP) at a scan rate of 0.1 V s^{-1}. Spectroelectrochemical (SEC) measurements were performed to measure the UV-vis absorption spectra of the one electron reduced species (OER) of **4**, **5**, and **6** using strands of 0.1 mm diameter Pt wire. In a porous glass tube (2 mm i.d., 3 mm o.d., 40 mm length) as the working electrode, a Pt wire coiled around the porous glass tube as the counter electrode, and an $Ag/AgNO_3$ reference electrode. A THF solution containing **4**, **5**, and **6** (0.5 mM) and TBAP (0.1 M) in a quartz cell was purged with Ar for 10 minutes. Immediately after electrolysis using a BAS 100 electrochemical analyzer, the UV-vis absorption spectra were measured.

Crystal Structure Determination. Crystals of **1**, **2**, **3**, and **4** were obtained from toluene, sealed in glass capillaries under argon, and mounted on the diffractometer. Preliminary examination and data collection were performed using a Bruker SMART CCD detector system single-crystal X-ray diffractometer equipped with a sealed-tube X-ray source (40 kV × 50 mA) using graphite-monochromated Mo Kα radiation (λ = 0.71073 Å). Preliminary unit cell constants were determined with a set of 45 narrow-frame (0.3° in ϖ) scans. The double-pass method of scanning was used to exclude any noise. The collected frames were integrated using an orientation matrix determined from the narrow-frame scans. The *SMART* software package was used for data collection, and *SAINT* was used for frame integration. Final cell constants were determined by a global

refinement of *xyz* centroids of reflections harvested from the entire data set. Structure solution and refinement were carried out using the *SHELXTL-PLUS* software package.

Density Functional Calculations. All calculations were performed with the *Gaussian 09* package to perform the geometry optimizations, spectra analysis, and excited state evaluations. The ground-state geometries of all compounds, as well as their cationic and anionic molecules, were optimized at the density function theory (DFT) level. The characterization of the low-lying excited singlet states relies on the time-dependent DFT (TD-DFT) calculation that is performed on the basis of the ground-state geometry by B3LYP density functional theory (DFT), using a 6-31G basis set. The various properties of all compounds, such as HOMOs, LUMOs, energy gaps, ionization potentials, electron affinities, and reorganization energies are obtained from the computed results and are compared to the available experimental data.

Common procedure for the synthesis of boron-phenylated o-carborane (1−3). 1,2-Diphenyl-o-carborane (1.48 g, 5.0 mmol) was added to a solution of KOH (0.84 g, 15 mmol) in 50 mL of ethanol and the clear reaction mixture was heated to reflux. TLC of the reaction mixture sample showed no starting material spot after that time. The reaction mixture was evaporated to dryness and re-dissolved in 50 mL of distilled water. Excess of Me_4NCl was added to the reaction mixture and the precipitate of tetramethylammonium nido-carborane salt formed was filtered off and dried by air suction (1.80 g, 100%). A 2.5 M solution of n-BuLi in hexane (1.0 mL, 2.2 mmol) was slowly added dropwise to a stirred solution of tetramethylammonium nido-carborane salt (0.72 g, 2.0 mmol) in 40 mL of THF at −78 °C. The reaction mixture was stirred at −78 °C for 1 h. A solution of dichlorophenylborane (0.35 g, 2.2 mmol) in 10 mL

of distilled THF was added via cannula. After this addition the reaction mixture was allowed to warm to room temperature and then heated to reflux 6 h. The white precipitate of lithium chloride was removed by filtration in air and washed on the filter with THF. After evaporation the crude reaction mixture was purified by column chromatography (Hx eluent) to give 1,2,3-triphenyl-o-carborane **1** then recrystallized from hexane to obtain as white powder. Yield: 86% (0.64 g, 1.72 mmol). m.p.: 193-194 °C. HRMS: Calcd for $[^{12}C_{20}{}^{11}B_{10}{}^{1}H_{24}]^{+}$ 374.2809. Found: 374.2802. IR spectrum (KBr pellet, cm^{-1}): ν(B−H) 2581, 2601; ν(C−H) 3237. ^{1}H NMR ($CDCl_3$, 600.1 MHz) δ 7.410 (m, 4H, Ph-H), 7.310 (m, 3H, Ph-H), 7.150 (m, 8H, Ph-H). ^{13}C NMR ($CDCl_3$, 150.9 MHz) δ 135.6, 131.3, 131.0, 129.9, 128.9, 128.0, 127.36 (Ph), 83.6 (Ph-Ccab). ^{11}B NMR ($CDCl_3$, 192.6 MHz) δ −1.62 (1B), −2.99 (3B), −8.02 (3B), −8.57 (2B), −10.15 (1B).

1,3,6-Triphenyl o-carborane (2). 1-Phenyl-o-carborane (1.10 g, 5.0 mmol) was added to a solution of KOH (0.84 g, 15 mmol) in 50 mL of ethanol and the clear reaction mixture was heated to reflux. TLC of the reaction mixture sample showed no starting material spot after that time. The reaction mixture was evaporated to dryness and re-dissolved in 50 mL of distilled water. Excess of Me4NCl was added to the reaction mixture and the precipitate of tetramethylammonium nido-carborane salt formed was filtered off and dried by air suction (1.42 g, 100%). A 2.5 M solution of n-BuLi in hexane (1.0 mL, 2.2 mmol) was slowly added dropwise to a stirred solution of tetramethylammonium nido-carborane salt (0.57 g, 2.0 mmol) in 40 mL of THF at −78 °C. The reaction mixture was stirred at −78 °C for 1 h. A solution of dichlorophenylborane (0.35 g, 2.2 mmol) in 10 mL of distilled THF was added via cannula. After this addition the reaction mixture was allowed to warm to room

temperature and then heated to reflux 6 h. The white precipitate of lithium chloride was removed by filtration in air and washed on the filter with THF. 1,3-Diphenyl-o-carborane (1.48 g, 5.0 mmol) was added to a solution of KOH (0.84 g, 15 mmol) in 50 mL of ethanol and the clear reaction mixture was heated to reflux. TLC of the reaction mixture sample showed no starting material spot after that time. The reaction mixture was evaporated to dryness and re-dissolved in 50 mL of distilled water. Excess of Me_4NCl was added to the reaction mixture and the precipitate of tetramethylammonium nido-carborane salt formed was filtered off and dried by air suction (1.80 g, 100%). A 2.5 M solution of n-BuLi in hexane (1.0 mL, 2.2 mmol) was slowly added dropwise to a stirred solution of tetramethylammonium nido-carborane salt (0.72 g, 2.0 mmol) in 40 mL of THF at −78 °C. The reaction mixture was stirred at −78 °C for 1 h. A solution of dichlorophenylborane (0.35 g, 2.2 mmol) in 10 mL of distilled THF was added via cannula. After this addition the reaction mixture was allowed to warm to room temperature and then heated to reflux 3 h. The white precipitate of lithium chloride was removed by filtration in air and washed on the filter with THF. After evaporation the crude reaction mixture was purified by column chromatography (Hx eluent) to give 1,3,6-triphenyl-o-carborane **2** then recrystallized from hexane to obtain as white powder. Yield: 58% (0.43 g, 1.2 mmol). m.p.: 178-179 °C. HRMS: Calcd for $[^{12}C_{20}{}^{11}B_{10}{}^{1}H_{24}]^+$ 374.2809. Found: 374.2819. IR spectrum (KBr pellet, cm^{-1}): ν(B−H) 2581, 2601; ν(C−H) 3237. ^{1}H NMR ($CDCl_3$, 600.1 MHz) δ 7.334 (d, 4H, J = 7.8 Hz), 7.218 (d, 1H, J = 7.2 Hz), 7.206 (d, 1H, J = 7.8 Hz), 7.129 (d, 2H, J = 7.2 Hz), 7.117 (d, 2H, J = 7.8 Hz), 7.001 (t, 1H, J = 7.2 Hz), 6.900 (d, 1H, J = 8.4 Hz), 6.887 (d, 1H, J = 7.2 Hz), 6.791 (d, 2H, J = 7.8 Hz), 4.433 (s, 1H). ^{13}C NMR ($CDCl_3$, 150.9 MHz) δ 133.7, 130.5, 129.2, 128.6, 127.7,

127.6, 127.1 (Ph), 78.3 (Ph-Ccab), 57.8 (H-Ccab). ^{11}B NMR ($CDCl_3$, 192.6 MHz) δ −0.88 (2B), −2.77 (1B), −4.82 (1B), −9.75 (2B), −11.04 (2B), −14.05 (2B).

1,2,3,6-Tetraphenyl o-carborane (3). Following the procedure described above for **1**, tetraphenylated-o-carborane **3** was prepared as a colorless crystal. Yield: 37% (0.33 g, 0.74 mmol). m.p.: 252-253 °C. HRMS: Calcd for $[^{12}C_{26}{}^{11}B_{10}{}^{1}H_{28}]^+$ 450.3122. Found: 450.3108. IR spectrum (KBr pellet, cm^{-1}): ν (B−H) 2581, 2601; ν (C−H) 3237. ^{1}H NMR ($CDCl_3$, 600.1 MHz) δ 7.294 (d, 4H, J = 7.8 Hz, Ph-H), 7.242 (d, 4H, J = 8.4 Hz, Ph-H), 7.229 (d, 4H, J = 7.8 Hz, Ph-H), 7.138 (d, 2H, J = 7.2 Hz, Ph-H), 7.126 (d, 2H, J = 7.8 Hz, Ph-H), 6.991 (t, 4H, J = 7.8 Hz, Ph-H). ^{13}C NMR ($CDCl_3$, 150.9 MHz) δ 134.6, 132.0, 130.2, 129.5, 128.9, 127.6, 127.1 (Ph), 80.3 (Ph-Ccab). ^{11}B NMR ($CDCl_3$, 192.6 MHz) δ 1.44 (2B), −2.75 (3B), −8.50 (2B), −9.45 (3B).

Reaction of $Cr(CO)_6$ with 2. Compound **2** (0.37 g, 1.0 mmol) and $[Cr(CO)_6]$ (0.44 g, 2.0 mmol) were dissolved in a mixture of THF (5 mL) and di-n-butyl ether (50 mL). The mixture was refluxed for 72 h and the resulting dark reddish solution was cooled to room temperature and filtered over Celite. The solvents were evaporated under reduced pressure. After evaporation the crude reaction mixture was purified by column chromatography (CH_2Cl_2:Hx eluent) to give chromium complex **4** then recrystallized from hexane to obtain as red crystals. Yield: 87% (0.59 g, 0.87 mmol). HRMS: Calcd for $[^{12}C_{28}{}^{1}H_{30}{}^{11}B_{10}{}^{52}Cr_2{}^{16}O_6]^+$ 676.1783. Found: 676.1768. IR spectrum (KBr pellet, cm^{-1}): ν (B−H) 2583, 2589; ν (CO) 1960, 1892. ^{1}H NMR ($CDCl_3$, 300.1 MHz) δ 7.62 (m, 4H, Ph-H), 7.47 (m, 3H, Ph-H), 7.30 (m, 8H, Ph-H). ^{13}C NMR ($CDCl_3$, 75.4 MHz) δ 231.4 (Cr-CO), 141.5, 137.9, 134.8, 132.7, 131.3, 130.8, 128.7 (Ph), 85.6

(Ph-Ccab). ^{11}B NMR ($CDCl_3$, 96.3 MHz) δ −1.84 (1B), −3.11 (3B), −8.54 (3B), −8.71 (2B), −10.37 (1B).

5. References

(1) (a) Weber, L.; Kahlert, J.; Brockhinke, R.; Böhling, L.; Brockhinke, A.; Stammler, H. -G.; Neumann, B.; Harder, B. A.; Fox, M. A. *Chem. Eur. J.* **2012**, *18*, 8347. (b) Ferrer-Ugalde, A.; Juárez-Pérez, E. J.; Teixidor, F.; Viñas, C.; Sillanpää, R.; Pérez-Inestrosa, E.; Núñez, R. *Chem. Eur. J.* **2012**, *18*, 544. (c) González-Cardoso, P.; Stoica, A. -I.; Farràs, P.; Pepiol, A.; Viñas, C.; Teixidor, F. *Chem. Eur. J.* **2010**, *16*, 6660. (d) Tsuji, M. *J. Org. Chem.* **2004**, *69*, 4063.

(2) (a) Fox, M. A.; Nervi, C.; Crivello, A.; Batsanov, A. S.; Howard, J. A. K.; Wade, K.; Low, P. J. *J. Solid State Electrochem.* **2009**, *13*, 1483. (b) Fox, M. A.; Nervi, C.; Crivello, A.; Low, P. J. *Chem. Commun.* **2007**, 2372.

(3) Hawthorne, M. F.; Wegner, P. A. *J. Am. Chem. Soc.* **1968**, *90*, 896.

(4) (a) Safronov, A. V.; Sevryugina, Y. V.; Jalisatgi, S. S.; Kennedy, R. D.; Barnes, C. L.; Hawthorne, M. F. *Inorg. Chem.* **2012**, *51*, 2629. (b) Holub, J.; Bakardjiev, M.; Štíbr, B.; Štěpnička, P.; Císařová, I. *E. J. Inorg. Chem.* **2010**, 4196.

(5) (a) Fox, M. A.; Peace, R. J.; Clegg, W.; Elsegood, M. R. J.; Wade, K. *Polyhedron* **2009**, *28*, 2359. (b) Boyd, L. A.; Clegg, W.; Copley, R. C. B.; Davidson, M. G.; Fox, M. A.; Hibbert, T. G.; Howard, J. A. K.; Mackinnon, A.; Peace, R. J.; Wade, K. *Dalton Trans.* **2004**, 2786.

(6) (a) Kokado, K.; Chujo, Y. *Dalton Trans.* **2011**, *40*, 1919. (b) Kokado, K.; Chujo, Y. *J. Org. Chem.* **2011**, *76*, 316. (c) Kokado, K.; Nagai, A.; Chujo, Y. *Tetrahedron Lett.* **2011**, *52*, 293.

(7) Henly, T. J.; Knobler, C. B.; Hawthorne, M. F. *Organometallics* **1992**, *11*, 2313.

(8) (a) Oliva, J. M.; Allan, N. L.; Schleyer, P. v. R.; Viñas, C.; Teixidor, F. *J. Am. Chem. Soc.* **2005**, *127*, 13538. (b) Llop, J.; Viñas, C.; Oliva, J. M.; Teixidor, F.; Flores, M. A.; Kivekas, R.; Sillanpää, R. *J. Organomet. Chem.* **2002**, *657*, 232.

6. Figures

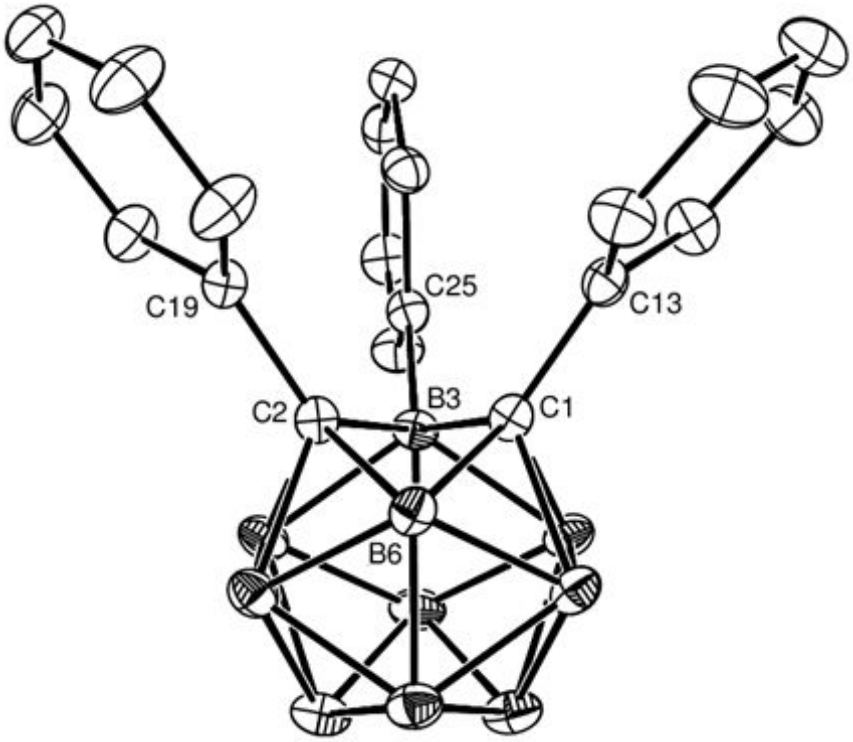

Figure 3. X-ray crystal structure of 1,2,3-Triphenyl-*o*-carborane.

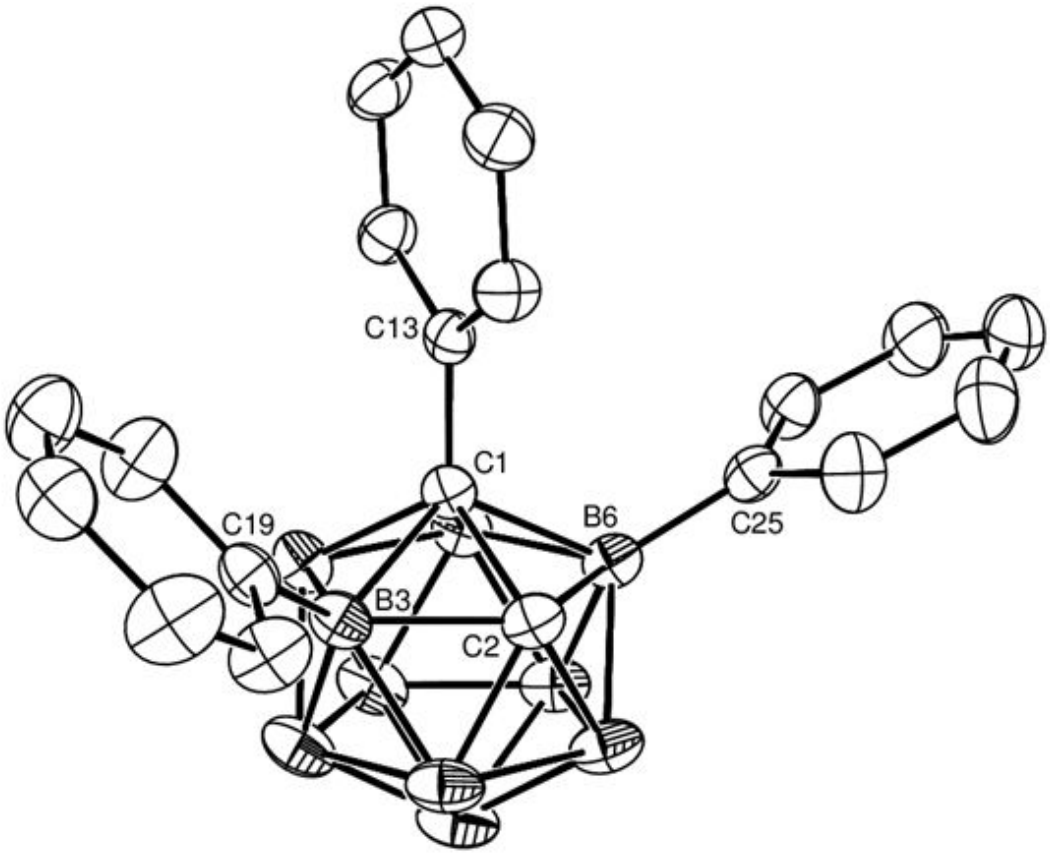

Figure 4. X-ray crystal structure of 1,3,6-Triphenyl-*o*-carborane.

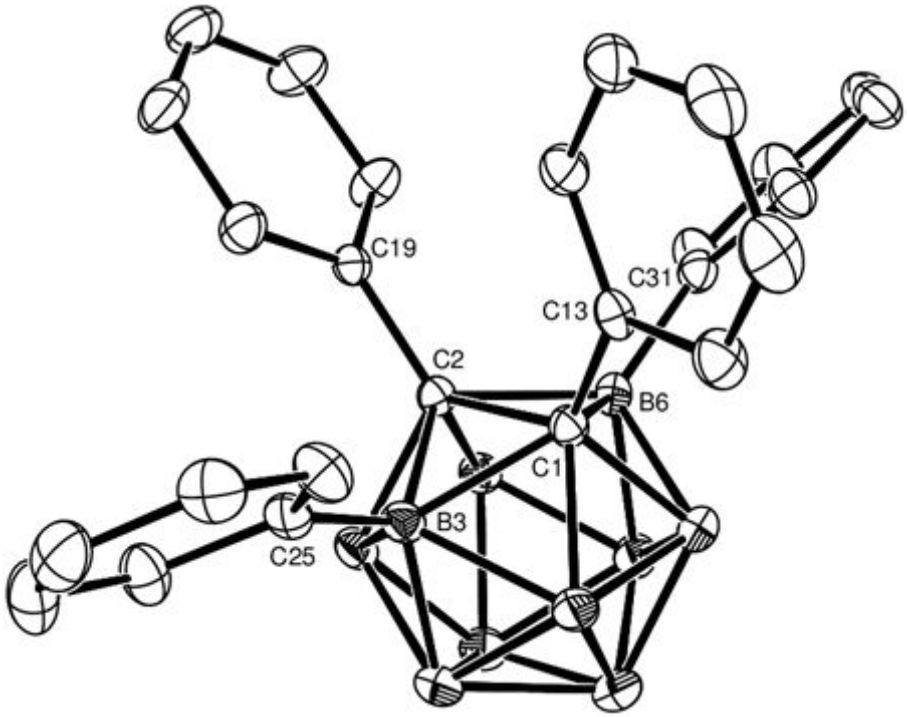

Figure 5. X-ray crystal structure of 1,2,3,6-Triphenyl-*o*-carborane.

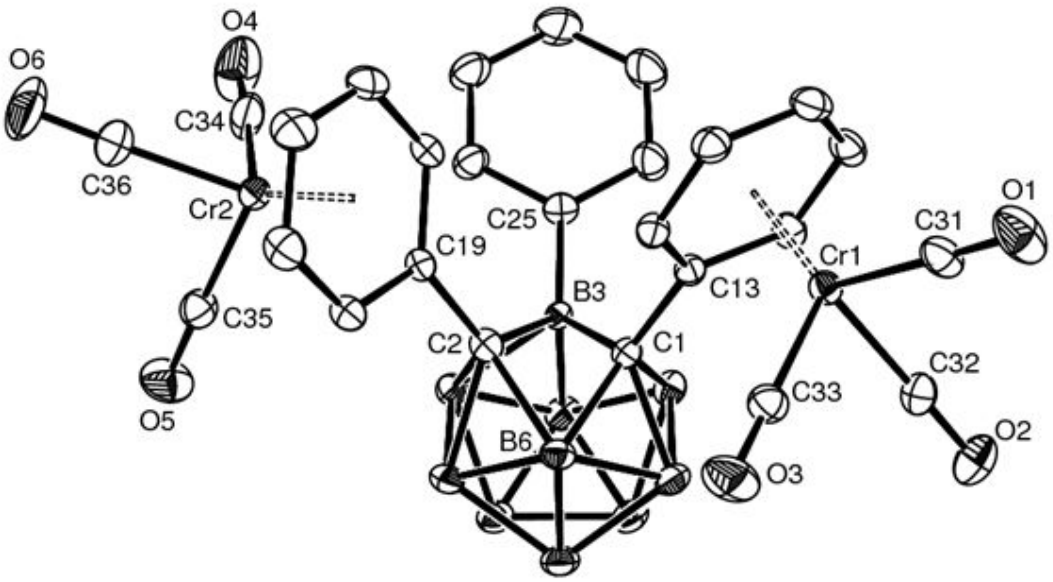

Figure 6. X-ray crystal structure of Cr compound.

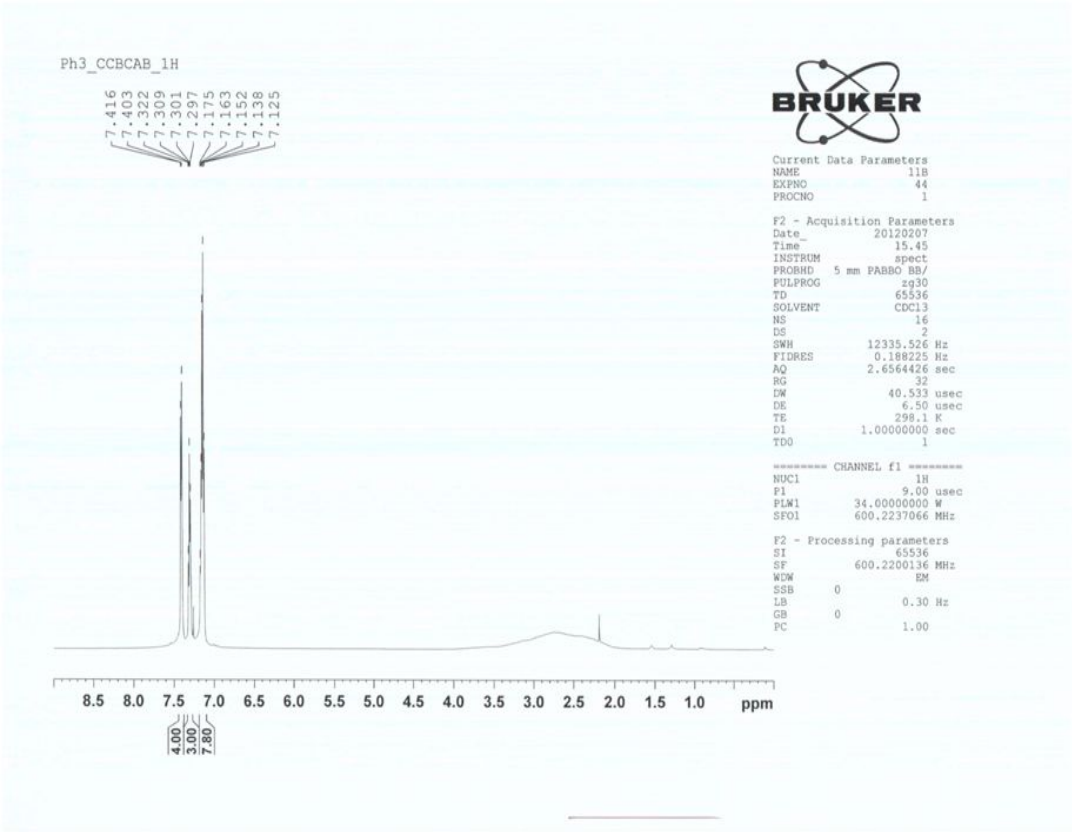

Figure 7. 1,2,3-Triphenyl-*o*-Carborane ^{1}H NMR.

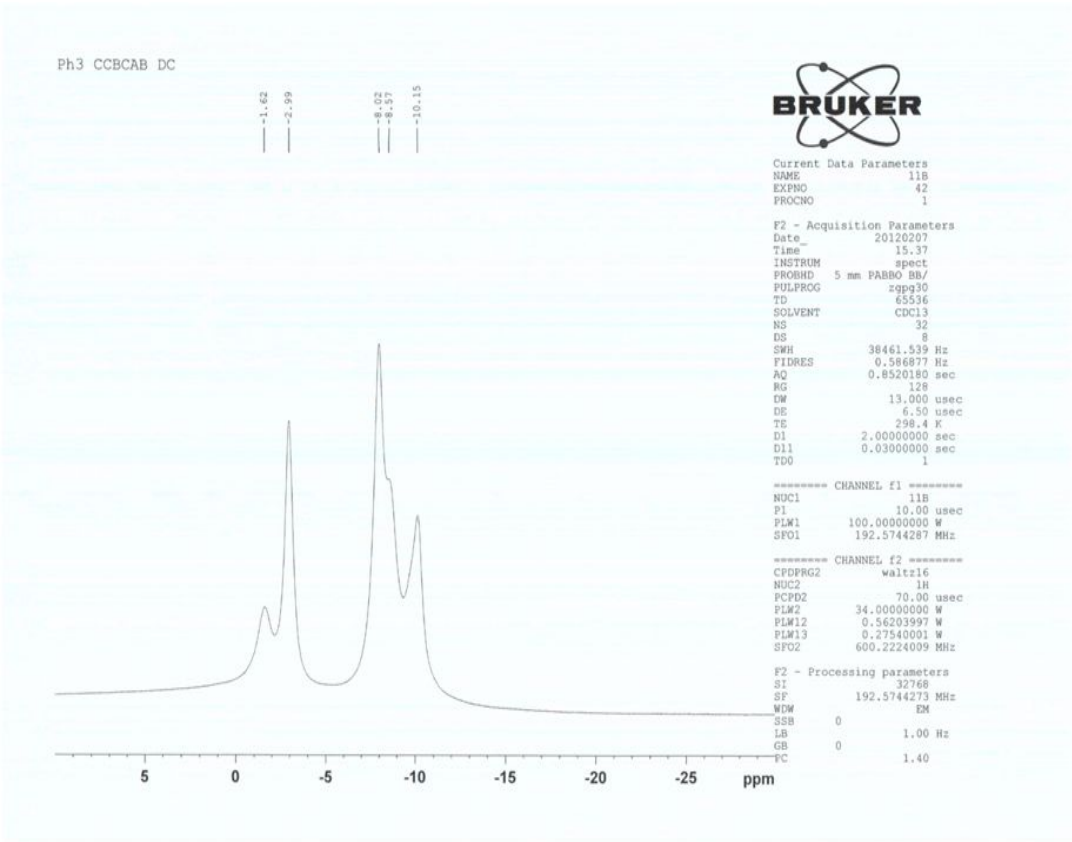

Figure 8. 1,2,3-Triphenyl-*o*-Carborane $^{11}B\{^{1}H\}$ NMR.

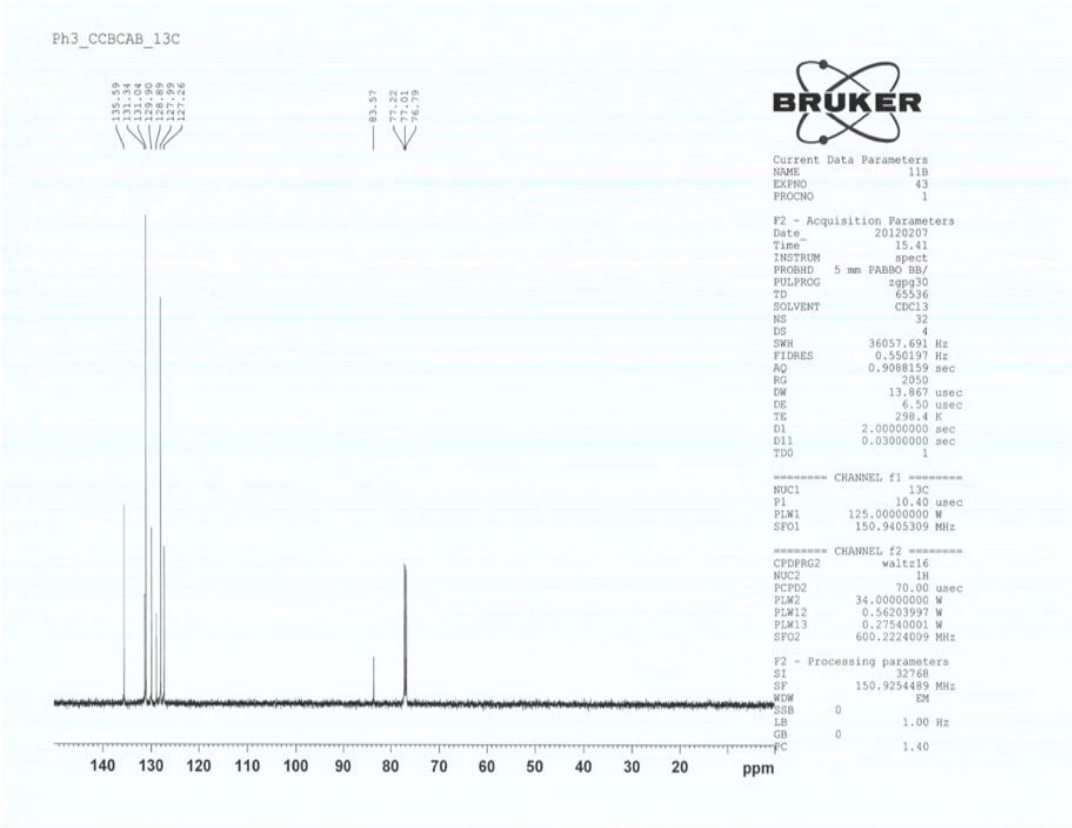

Figure 9. 1,2,3-Triphenyl-*o*-Carborane ^{13}C NMR.

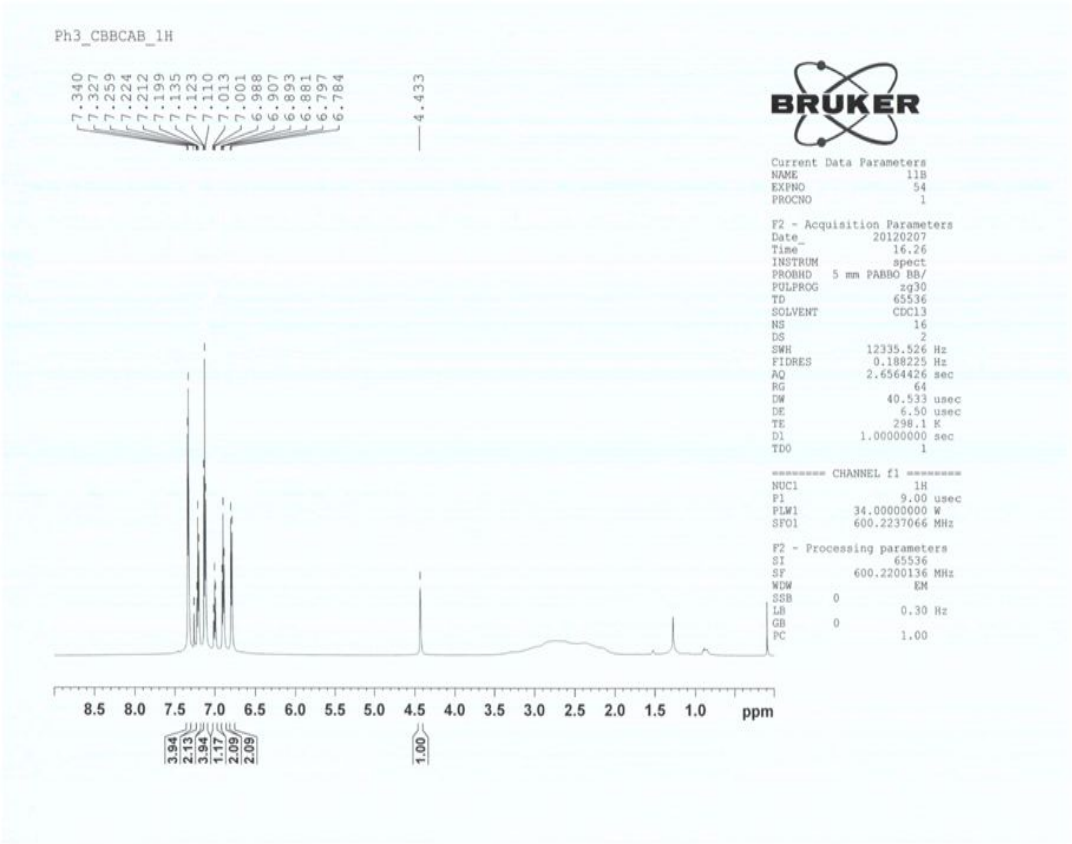

Figure 10. 1,3,6-Triphenyl-*o*-Carborane ^{1}H NMR.

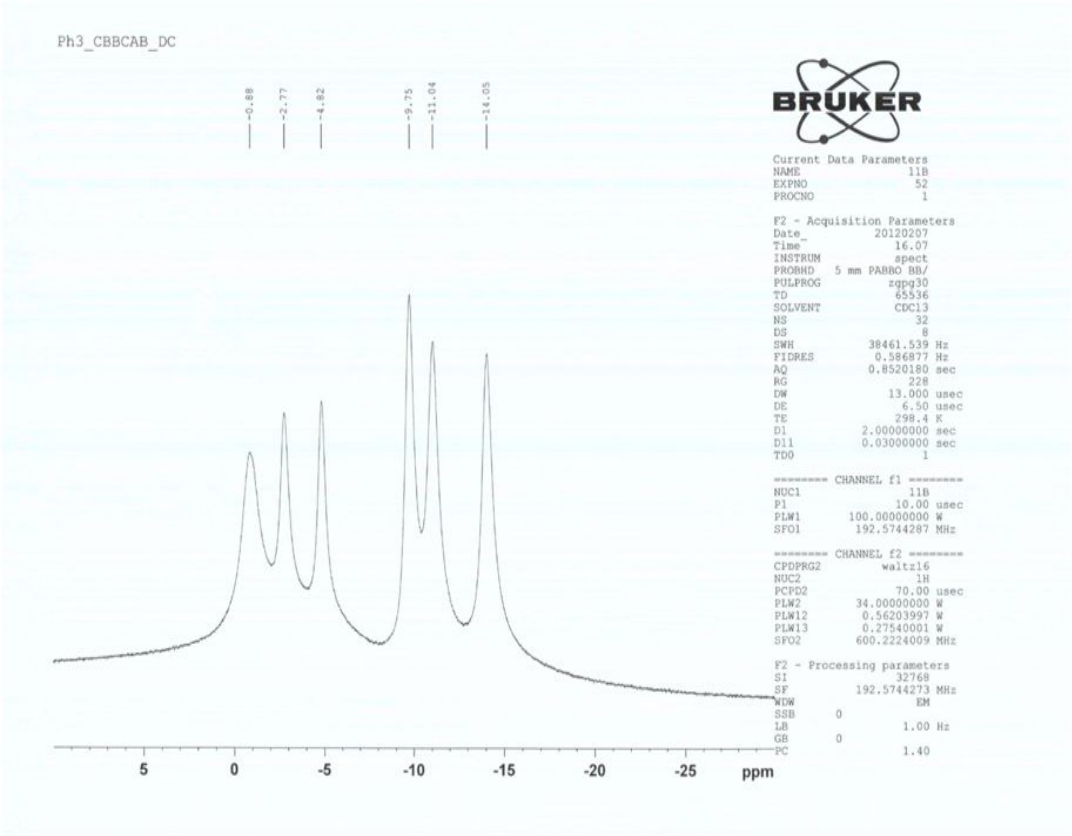

Figure 11. 1,3,6-Triphenyl-*o*-Carborane $^{11}B\{^{1}H\}$ NMR.

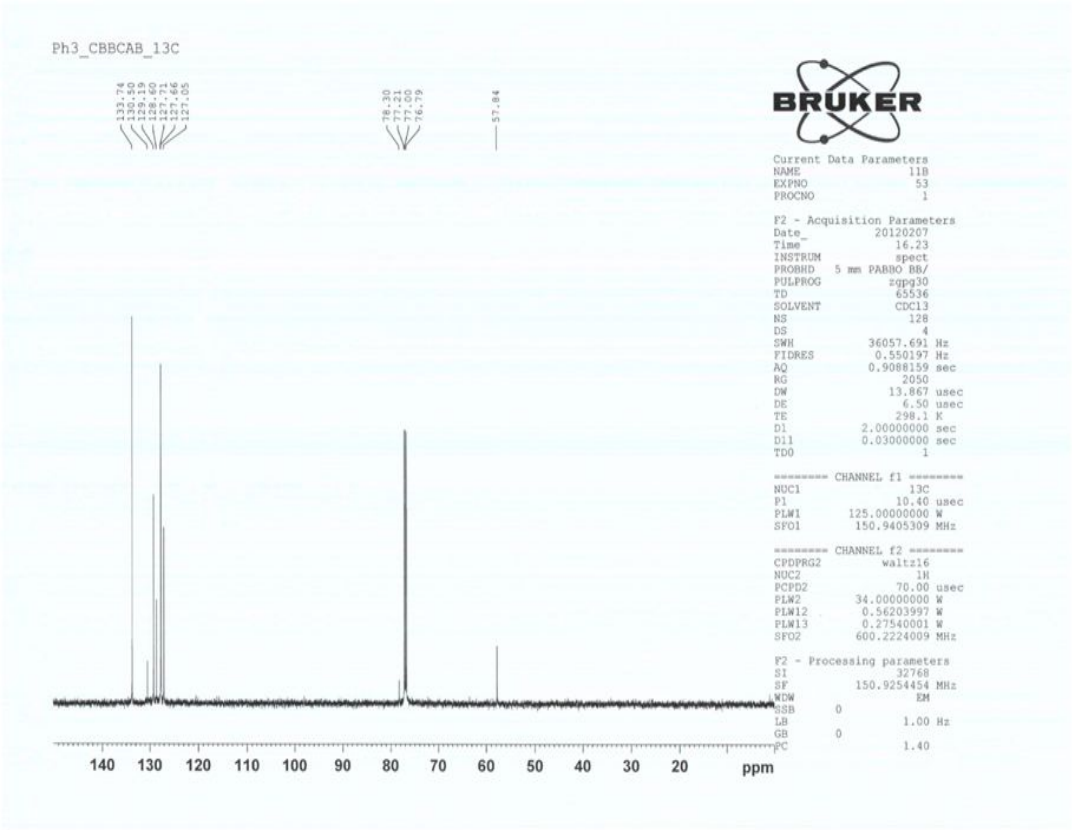

Figure 12. 1,3,6-Triphenyl-*o*-Carborane ^{13}C NMR.

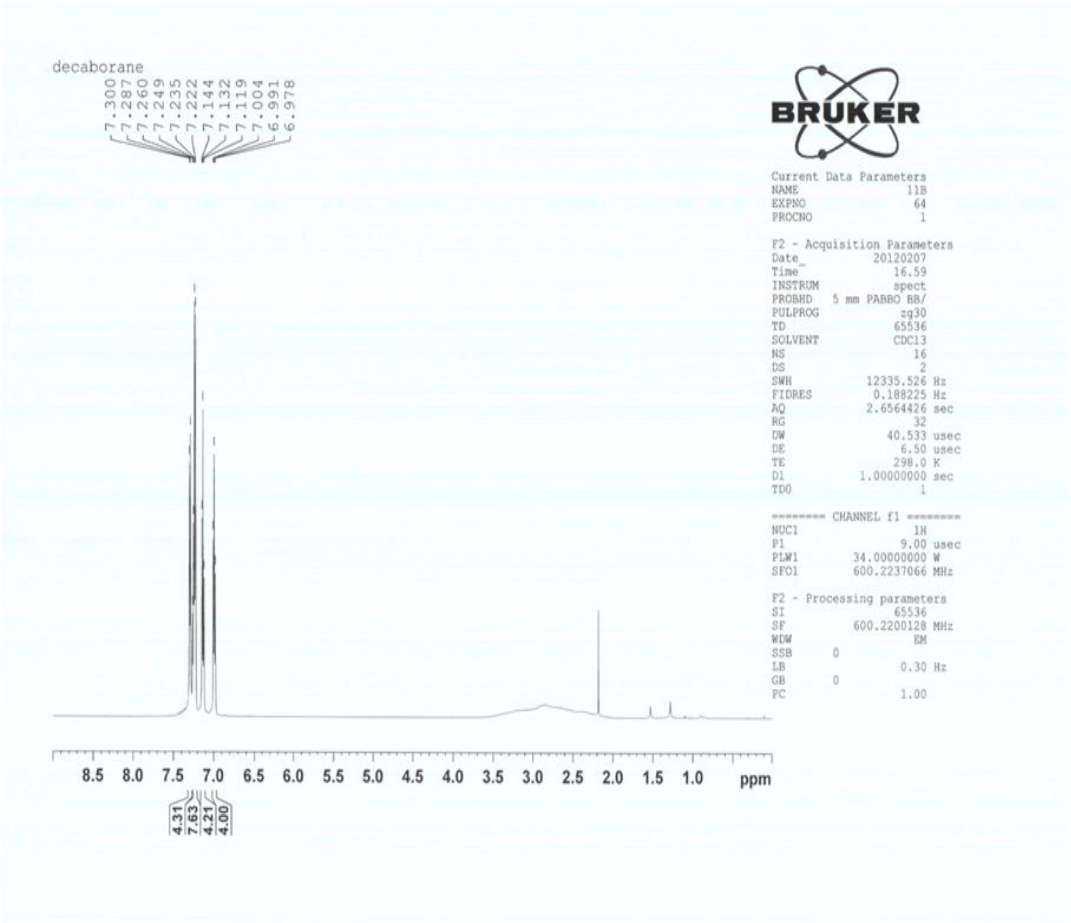

Figure 13. 1,2,3,6-Tetraphenyl-*o*-Carborane ^{1}H NMR.

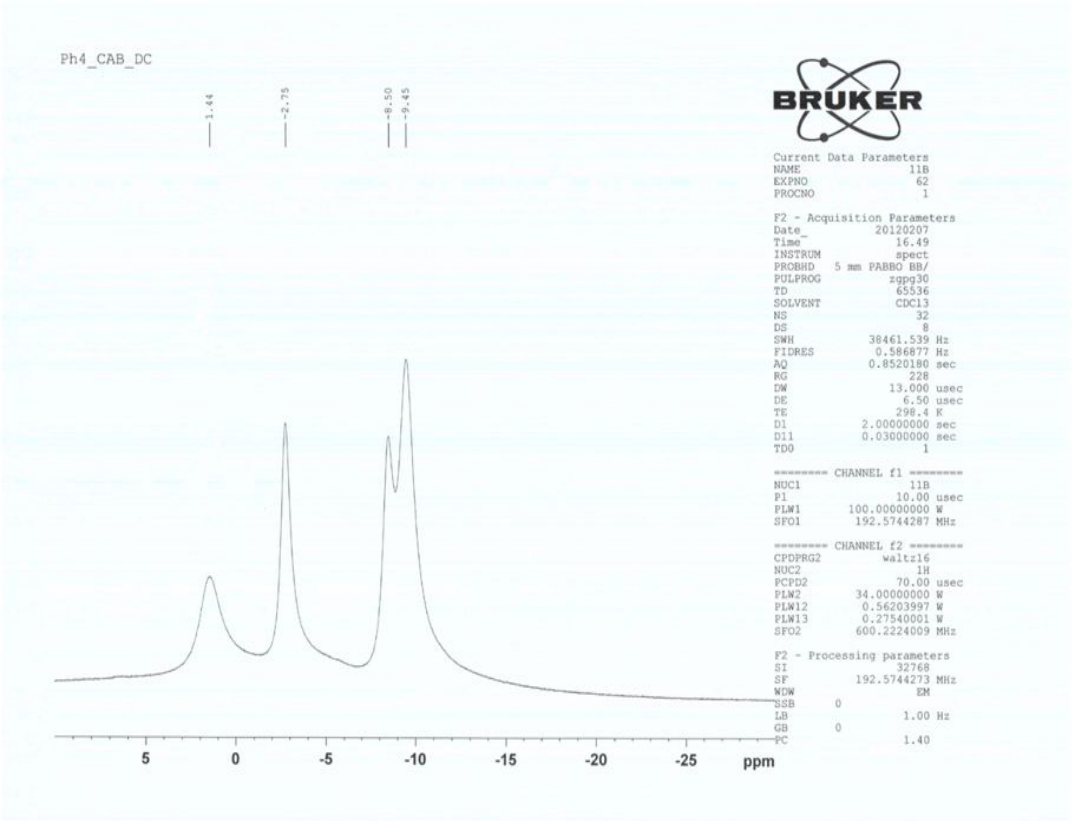

Figure 14. 1,2,3,6-Tetraphenyl-*o*-Carborane $^{11}B\{^{1}H\}$ NMR.

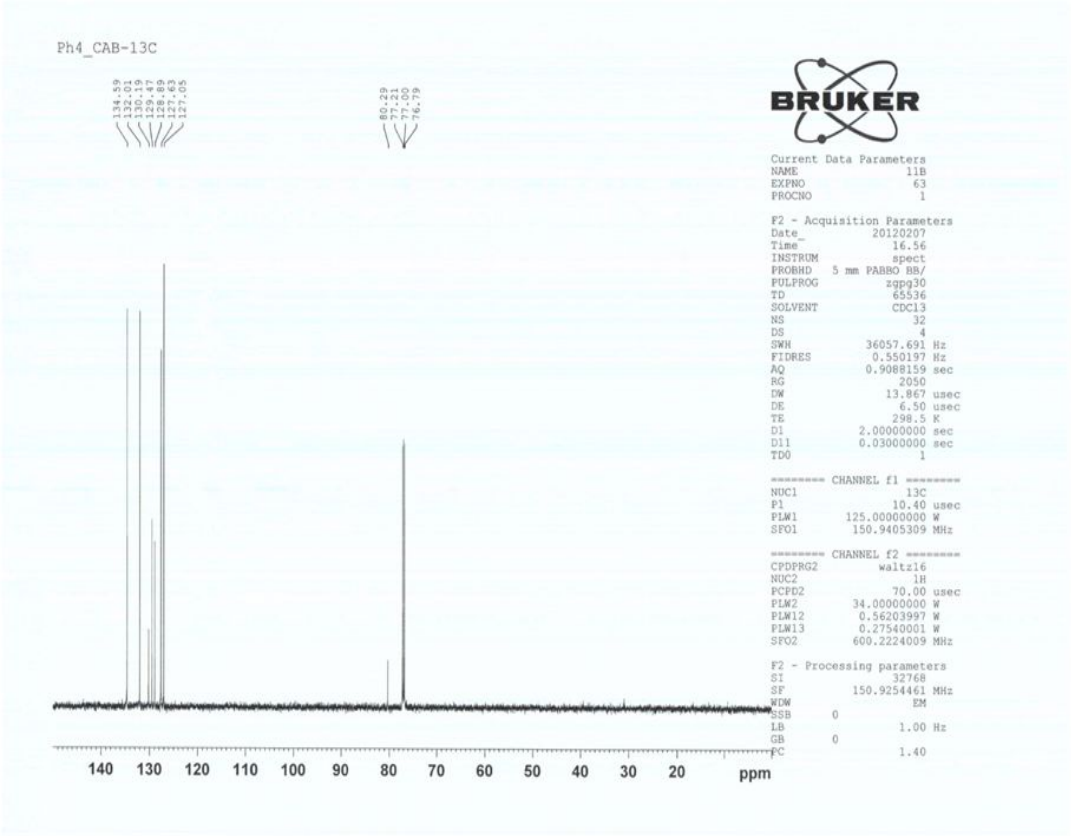

Figure 15. 1,2,3,6-Tetraphenyl-*o*-Carborane ^{13}C NMR.

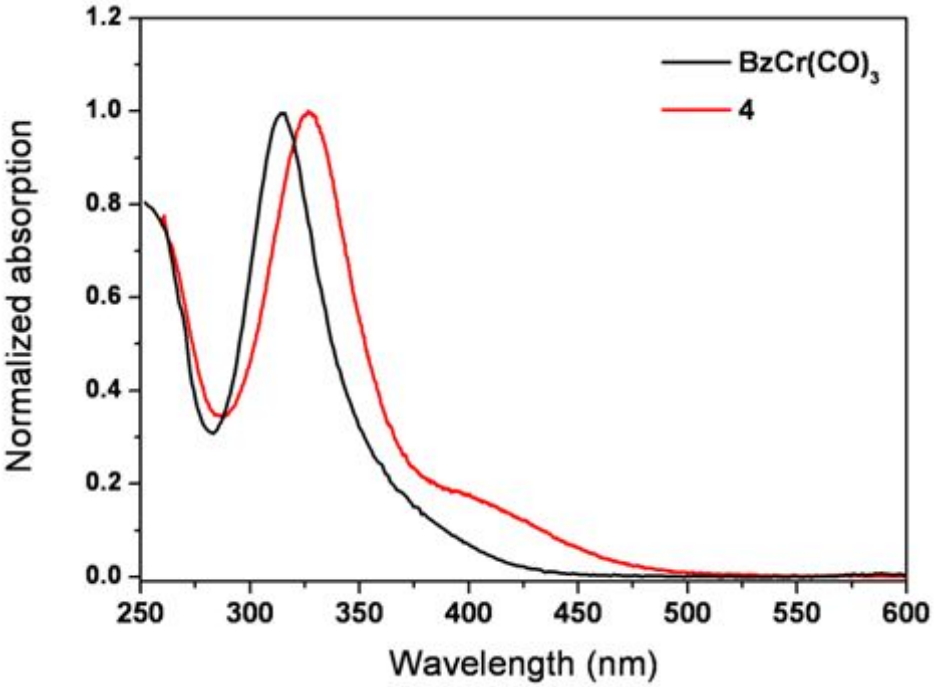

Figure 16. UV-vis absorption spectrum of **BzCr(CO)$_3$** and **4** in hexane solution at room temperature.

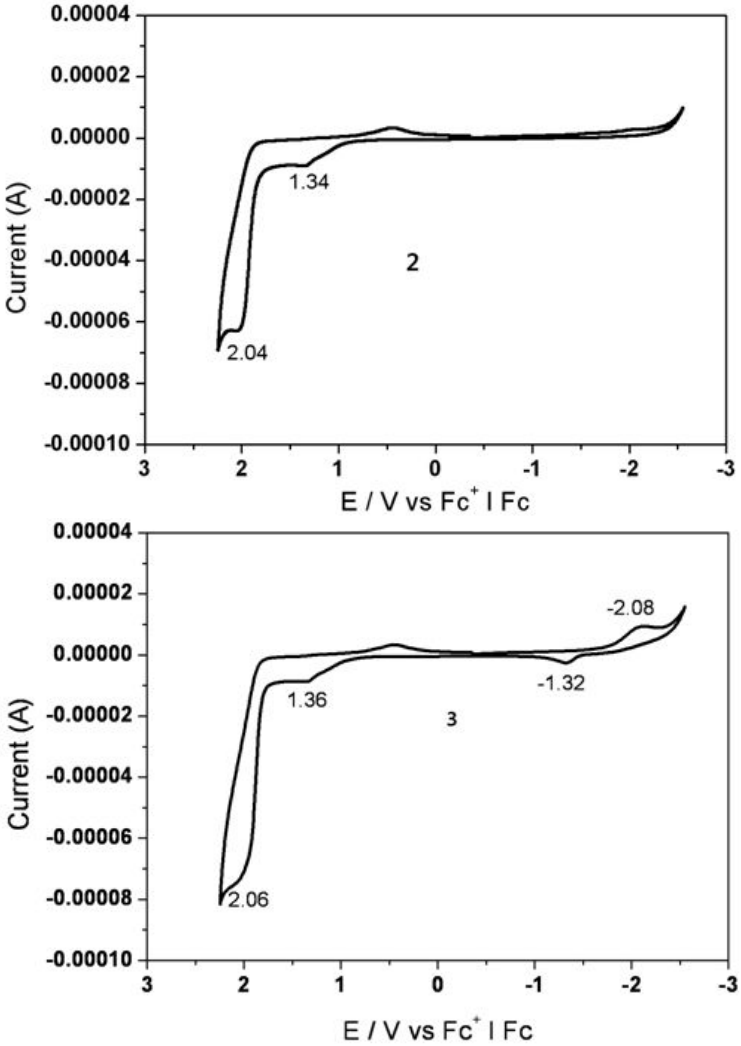

Figure 17. Cyclic Voltammometry for (top) **2** and (bottom) **3** (TBAP (0.1 M)/sample (1 mM), Scan rate: 100 mV/s, Solvent: CH_2Cl_2).

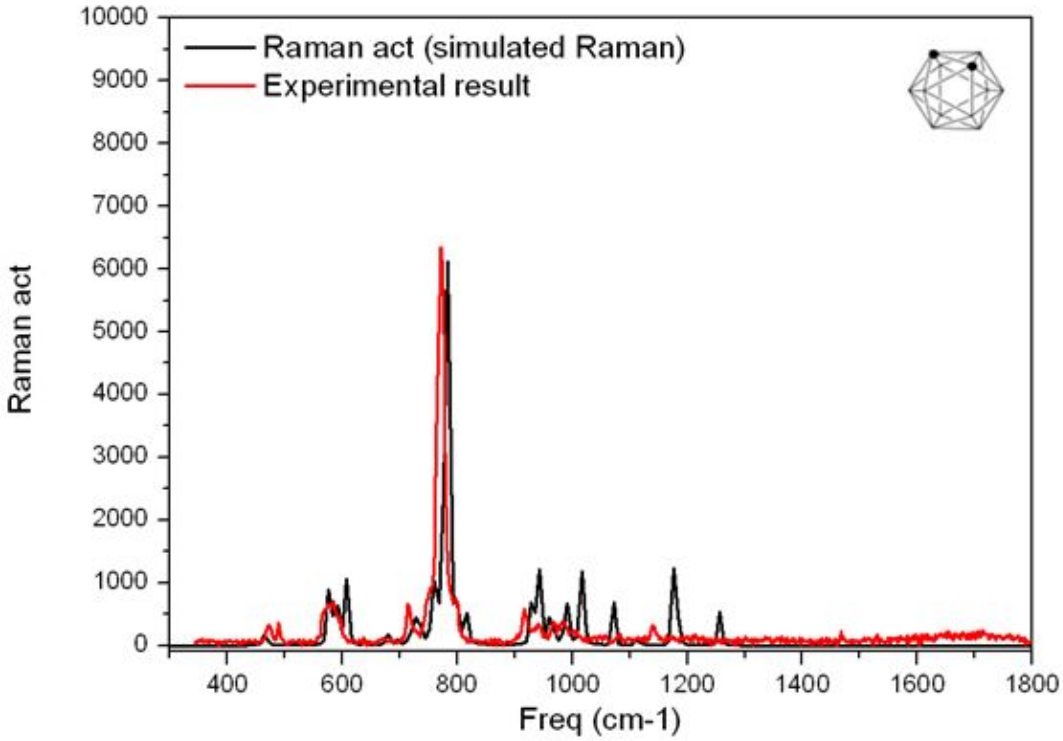

Figure 18. Simulated and experimental Raman spectra of *o*-carborane at room temperature.

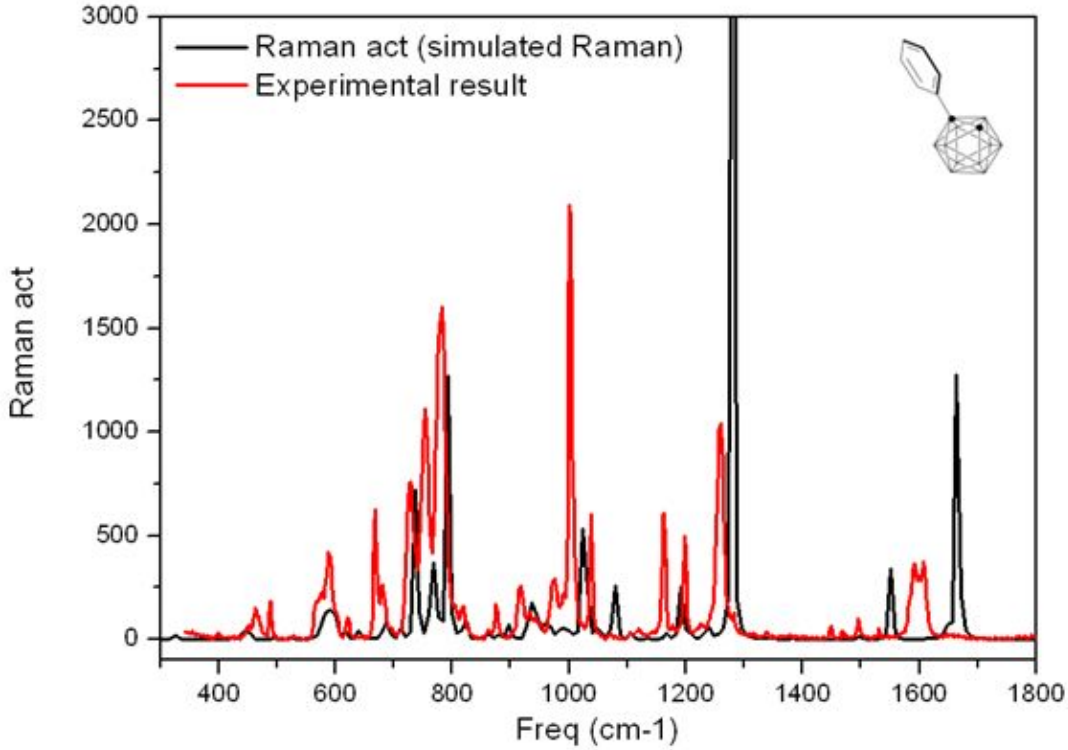

Figure 19. Simulated and experimental Raman spectra of phenyl-*o*-carborane at room temperature.

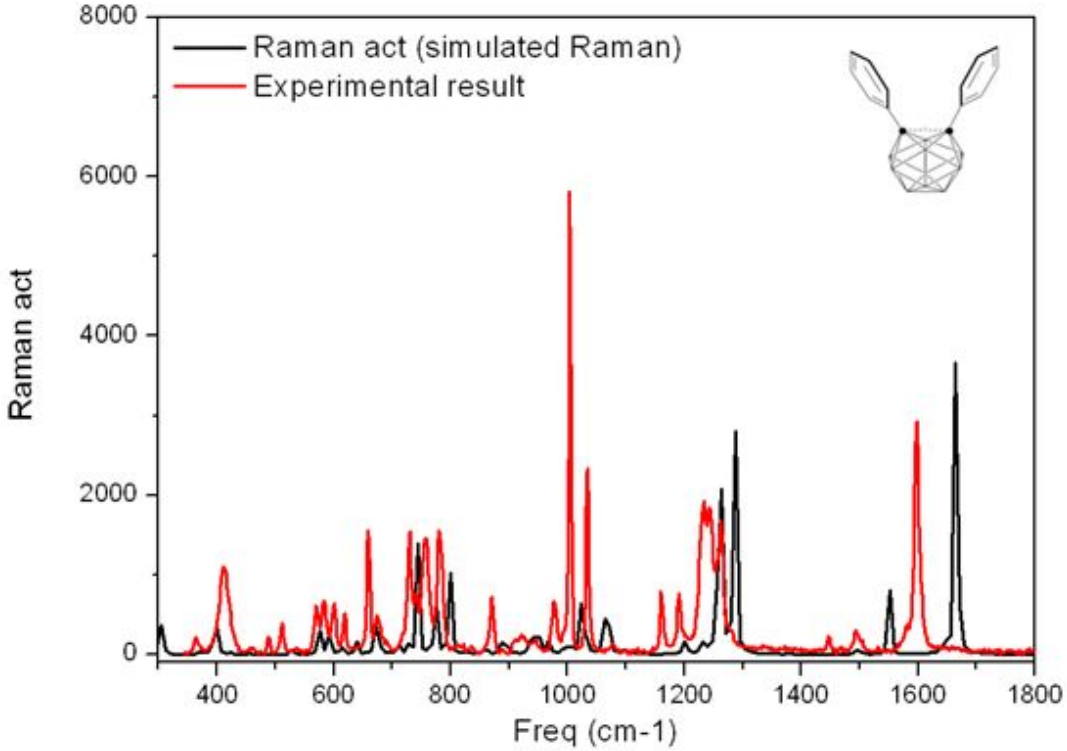

Figure 20. Simulated and experimental Raman spectra of diphenyl-*o*-carborane at room temperature.

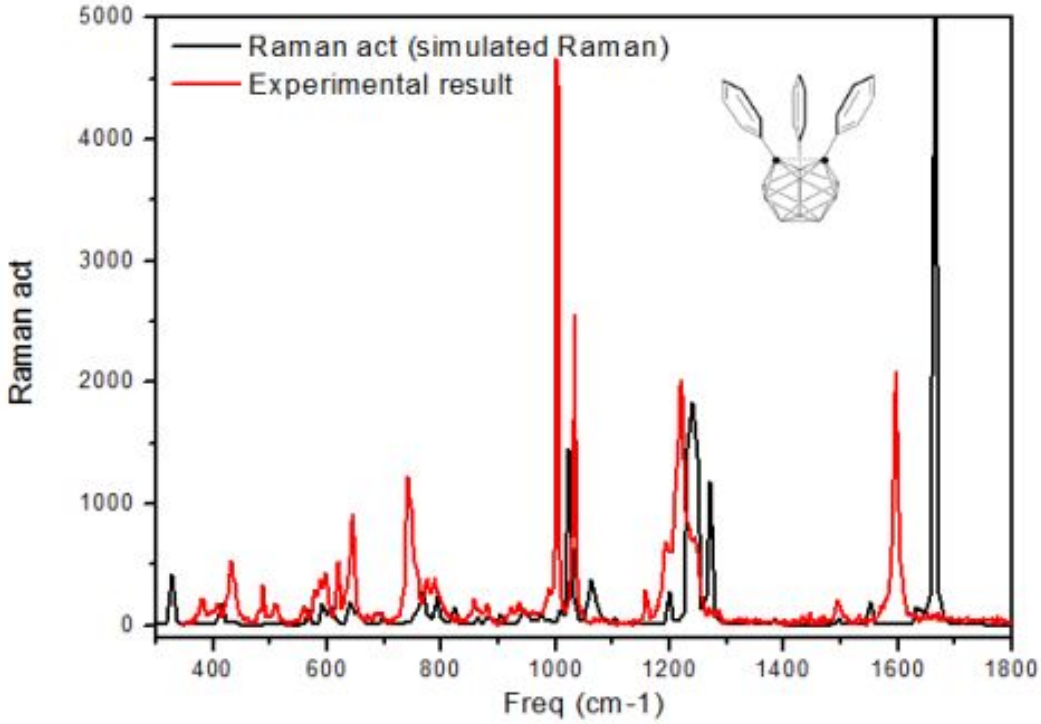

Figure 21. Simulated and experimental Raman spectra of 1,2,3-Triphenyl-*o*-carborane at room temperature.

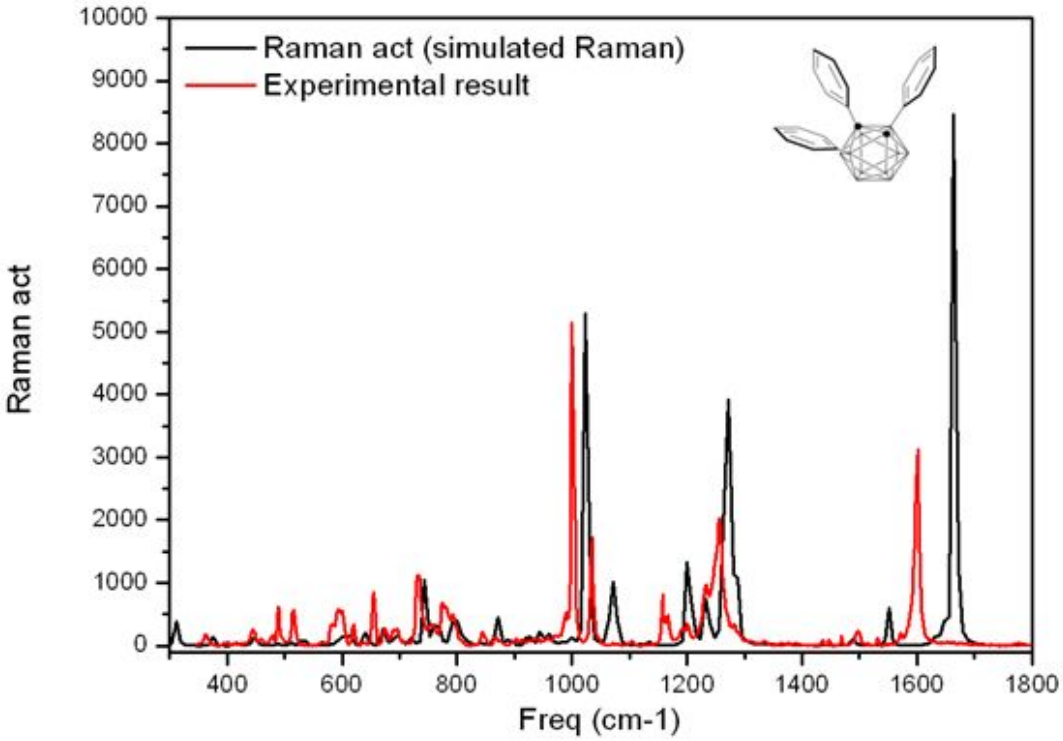

Figure 22. Simulated and experimental Raman spectra of 1,3,6-Triphenyl-*o*-Carborane at room temperature.

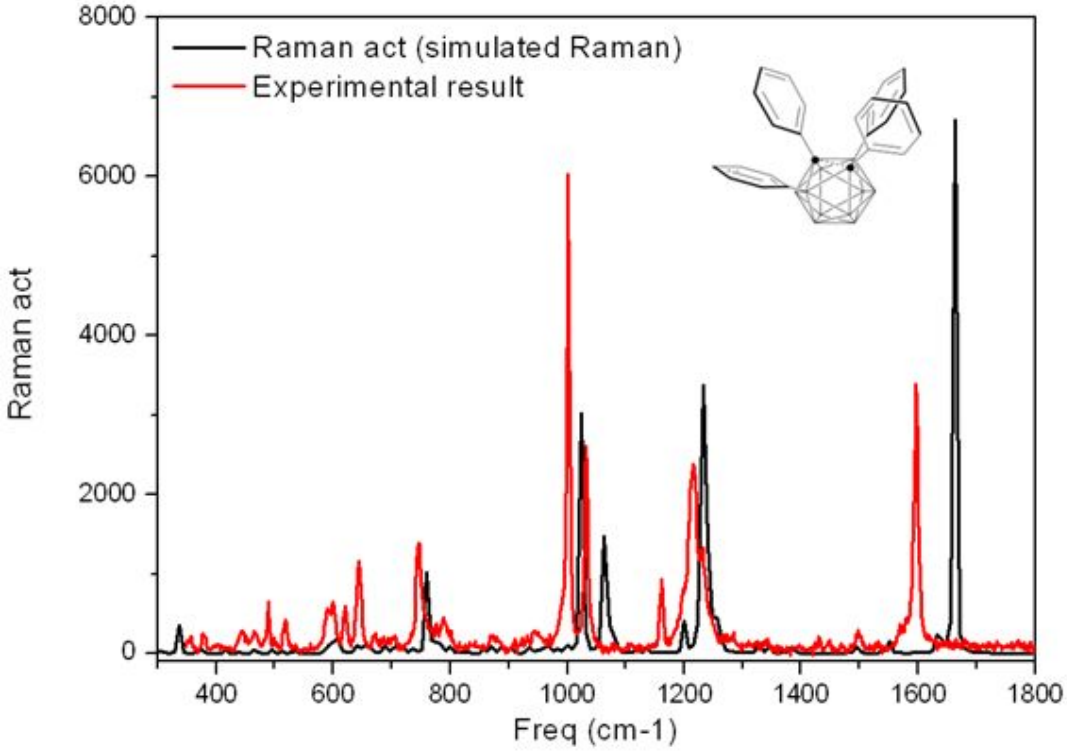

Figure 23. Simulated and experimental Raman spectra of 1,2,3,6-Tetraphenyl-*o*-Carborane at room temperature.

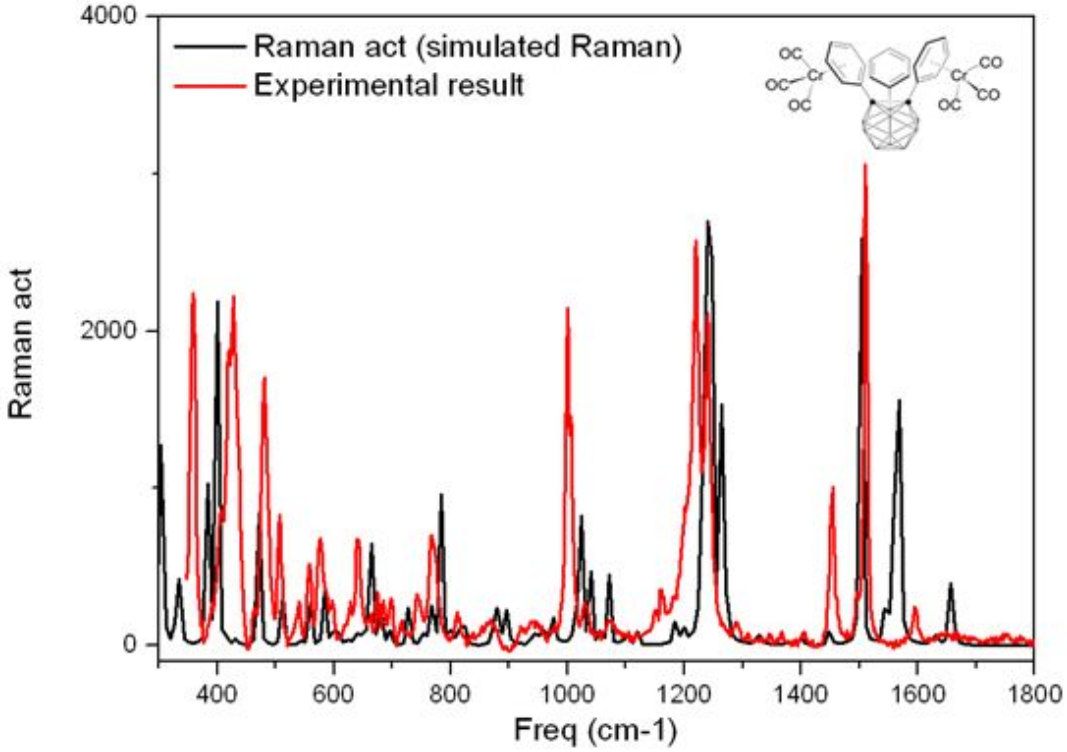

Figure 24. Simulated and experimental Raman spectra of Cr compound at room temperature.